Journal of Thermal Analysis and Calorimetry, Vol. 59 (2000) 617–624

CONTRIBUTION TO THE STUDY OF THE SOLID-STATE REACTION OF MERCURY WITH PURE RHODIUM

*E. Milaré, F. L. Fertonani**, *A. V. Benedetti and M. Ionashiro*

Instituto de Química, Universidade Estadual Paulista, Araraquara, São Paulo, C. P. 355
CEP 14.800-900, Brazil

Abstract

Thermogravimetry (TG) and other analysis techniques (EDX, SEM, Mapping surface, X-ray diffraction, inductively coupled argon plasma emission spectroscopy and atomic spectrometry with cold vapor generation) were used to study the reaction of Hg with Rh. The results permitted the suggestion that, when subjected to heat, an electrodeposited Hg film reacts with Rh to form intermetallic products with different stabilities, as indicated by at least three mass loss steps. In the first step, between room temperature and 160°C, only the bulk Hg is removed. From this temperature up to about 175°C, the mass loss can be attributed to the desorption of a film of metallic Hg. The last step, from 175 to 240°C, can be ascribed to the removal of Hg from a thin dark film of $RhHg_2$.

Keywords: EDX microanalysis, electrodeposit, mercury, rhodium, SEM, TG

Introduction

In recent work, Rh, Pt, Ir and their alloys have been used for many technological applications: as catalysts supported on alumina in the petroleum cracking industry [1]; on SiC as support in exhaust catalysis [2]; on SiO_2 and TiO_2 in automotive exhaust gas oxidation of NO to NO_2 and of SO_2 to SO_3 [3, 4]; as chemical catalysts in ammonia oxidation plants [5]; in many electrical devices [6]; and as micro- and ultramicroelectrodes in electrochemistry [7, 8]. Hg readily interacts with these noble metals and their alloys [9–12, 14], which can be an advantage or a disadvantage, depending on the application of the resulting material. Thus, as Hg may be present as a contaminant in petroleum, some problems arise, mainly in consequence of the formation of solid intermetallic compounds, since they can modify the catalytic properties in petroleum cracking processes. On the other hand, Pt, Hg and other metals can be electrodeposited on thin-film conductive diamond surfaces to produce novel catalytic electrodes, sensors and detectors [6]. The interaction of Hg with pure Pt has been investigated by means of cyclic voltammetry [13], X-ray diffraction and thermoanalytical techniques [14, 15] and thermogravimetry (TG) [16, 25].

* Author for correspondence: e-mail: fertonan@iq.unesp.br

1418–2874/2000/ $ 5.00

Akadémiai Kiadó, Budapest
Kluwer Academic Publishers, Dordrecht

The formation of a PtHg alloy and a solid solution (up to 0.23 Hg atoms per Pt atom) has been suggested [15] and the formation of $PtHg_4$ was investigated by means of X-ray diffraction and electrochemical techniques [17, 25]. The formation of other compounds, such as $PtHg_2$, Pt_2Hg, Pt_3Hg and bulk Hg on platinum, has been mentioned [13]. The existence of Rh–Hg compounds such as $RhHg_5$, $RhHg_{4.65}$ and $RhHg_2$ that are stable over only a very narrow composition range has been postulated [10, 11]. Recent work indicated only the presence of $RhHg_2$ on the surface of the Pt $Rh_{(10\ mass\%)}$–Hg (electrodeposited) system [18]. This compound was characterized by X-ray diffraction techniques after the Hg had been eliminated by heating of the system up to 230°C in a TG experiment.

In the present work, films of Hg were electrodeposited on pure Rh foils and the thermal desorption of the Hg was investigated by using TG, EDX, SEM, Mapping surface, X-ray diffraction, inductively coupled argon plasma emission spectroscopy (ICP) and atomic absorption spectrometry with cold vapor generation.

Experimental

Pure Rh foils with an area of 3 mm×20 mm and a thickness of 60 μm were prepared: they were polished with Al_2O_3 (particle size <0.3 μm) in aqueous suspension and washed in HNO_3:H_2O (50% v/v) in an ultrasonic bath. They were then submitted to the following heat treatments: a) heating at 1200°C for 4 h and quenching in oxygen-free water at 0°C. Each sample was treated with HNO_3:HCl (1:3 v/v) solution for 60 s and finally cleaned with a concentrated HF solution at 50°C for 24 h. For the electrochemical deposition of Hg on foils, a degassed solution containing 60 mmol Hg_2^{2+}+1M KNO_3+HNO_3 (pH 1) was used. The electrodeposition was performed by applying –0.46 V/ENH for 300 s to the stirred solution. These foils were washed several times by immersion in triply-distilled water, dried in a flux of N_2 and stored under a purified N_2 atmosphere.

TG curves were obtained at 5°C min^{-1}, in a flux of purified N_2 (150 cm^3 min^{-1}) from 30 to 800°C, using a Mettler Thermoanalyser TA-4000 system.

The sample surfaces, before and after heating to various temperatures, were examined by (JEOL, JSM-T330A), and EDX (Noran). The X-ray diffractograms were obtained with a Siemens D5000 instrument.

The data generated from the X-ray diffraction studies were treated with the software AFPAR (Complex des Programme, CNRS, France). This program was utilized to determine the lattice parameters of the possible species formed on the Rh foil surface. This method makes use of the experimental interplanar spacings (*d*-spacing), and data on an original prototype, such as $RhHg_2$ (values of lattice parameters and the respective reflections) [22], which were put together to obtain the experimental lattice parameters.

For Hg analysis a blank solution was prepared by treating pure Rh foils without electrodeposited Hg with 1 ml of concentrated HNO_3+5 drops of concentrated HCl in an ultrasonic bath; no Rh was detected in this solution.

The volumes of solutions produced by the immersion of Rh foils containing electrodeposited Hg, after treatment as above described, were adjusted to the desired

level with tridistilled water and a conserving solution (5% (v/v) HNO_3 and 0.01% $Cr_2O_7^{2-}$, added as either $K_2Cr_2O_7$ or CrO_3). Following addition of this conserving solution, samples containing ≥0.1 ng Hg ml^{-1} can be stored in glass without deterioration for as long as 5 months [19]. Hg was analyzed by atomic absorption spectroscopy via the cold vapor steam generation technique [20] in an Intralab-Varian, AA/1475 spectrometer, and Rh was analyzed by ICP with an ICP-AES (Sequential Espectroflame) spectrometer.

Results and discussion

Figure 1 shows the TG and DTG curves recorded on heating quenched pure Rh foil to 800°C. Although the TG curve indicates mass losses in two consecutive steps between 50 and ca 230°C, the DTG curve suggests three consecutive steps. The first mass loss observed in the TG curves occurs below 160°C in a very fast process that can be ascribed to the loss of Hg electrodeposited on Hg (bulk Hg). The quantity of Hg lost in this step corresponds to ca 61.4% of the total electrodeposited Hg. The resulting surface exhibits the aspect of a typical metallic surface, because the bulk Hg was not entirely eliminated. Figure 2a shows the SEM image of the surface of Rh after Hg electrodeposition and heating up to a temperature corresponding to the end of the first step in the TG curve. This SEM image reveals a surface covered by a film of metallic Hg and an absence of Hg at the grain boundaries.

The second step, observed between 160 and 175°C (Fig. 1) as a fast process, can be ascribed to the elimination of Hg present in a metallic Hg film. In this step, the mass loss was about 37.3% of the total Hg electrodeposited on the pure Rh foil. The resulting sur-

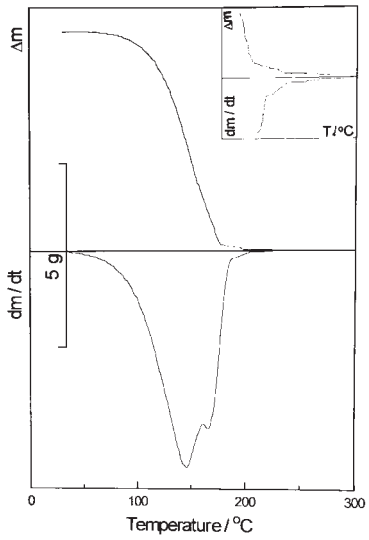

Fig. 1 TG and DTG curves for Rh foils containing electrodeposited Hg: heating rate, 5°C min^{-1}; N_2 flux (purified to remove traces of oxygen), 150 cm^3 min^{-1}; alumina crucible. Detail: amplification of the last step in the TG and DTG curves

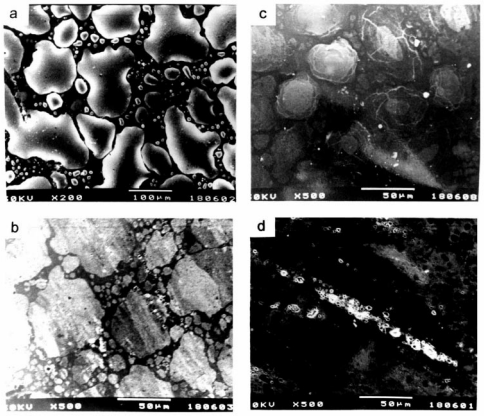

Fig. 2 SEM images of the Rh surface after Hg electrodeposition and heating up to: a – 160°C; amplificaton: 200 ×; b – 175°C; amplification: 500×; c – 230°C; amplification: 500×; and d – 800°C; amplification: 500×

face does not have a typically metallic surface because the bulk Hg has been eliminated. Figure 2b depicts the SEM image of the Rh after Hg electrodeposition and heating to a temperature corresponding to the end of the second step in the TG curve. This SEM image indicates a nearly smooth surface covered by a thin a grayish film, and reveals that the attack does not occur mainly at the grain boundaries. The presence of Hg on the Rh surface in this temperature range was confirmed by means of EDX microanalysis (Fig. 3), atomic absorption analysis (Table 1) and mapping surfaces (Figs 4a and b). For pure Rh, the results of EDX microanalysis demonstrate that the intensity of the Hg peaks decreases as the temperature is increased. However, the EDX microanalysis revealed a higher intensity at the center of the grain than at the grain boundaries.

Table 1 Flameless atomic absorption and atomic emission (AES-ICP) data for Hg and Rh after partial or total elimination of the Hg by heating up to different temperatures

Material	T/°C	m_i/mg	m(Hg)/mg	m(Rh)/mg
Rh	170	26.287	0.0561	0.00258
	230	28.932	0.00601	0.00573
	800	27.620	*	0.00403

*Below the detection limit; m_i: total initial mass

The last step, a slow process, was observed between 175 and 230°C, and can be ascribed to the elimination of Hg contained in a film, as a compound, probably $RhHg_2$. In this step, the mass loss was about 2.3%. It is well known that the reactivity of Hg with Pt is higher than that with Rh, and Hg does not react with Ir to form intermetallic species [12, 21]. In order to identify the reaction product present at the end of the second step in the TG curve, X-ray diffraction patterns were obtained. For this, a new sample was prepared as described in the Experimental section. The X-ray diffraction data obtained from the Rh foil surface after heating up to 175°C are shown

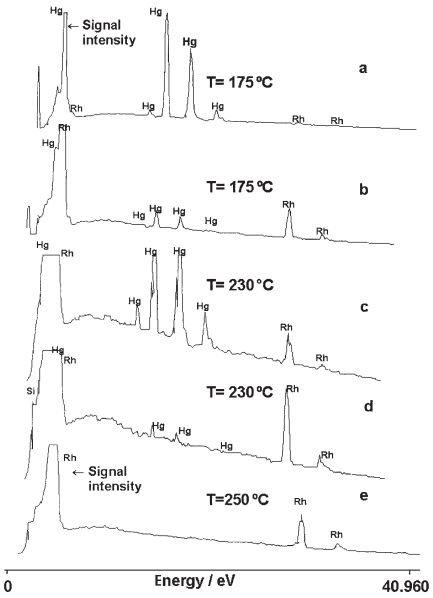

Fig. 3 EDX microanalysis of the Rh surface. *T*=175°C: a – center of grain – VFS: 4096; b – grain boundary – VFS: 2048; *T*=230°C: c – center of grain – VFS: 1024; d – grain boundary – VFS: 1024; *T*=300°C: e – general surface – VFS: 4096. Electron beam acceleration: 30 kV. Sample time: 300 s

in Table 2. Examination of the data shows that the diffraction lines correspond to Rh and $RhHg_2$. The absence of any diffraction peak from the other phases with higher Hg concentrations expected from the Rh–Hg phase diagram [11] indicates that their concentrations are negligible (less than a few percent).

Table 2 Identification of the diffraction peaks obtained on the Rh foil surface heated at 175°C

Compounds	2θ	*d*-spacing (exp.)	*d*-spacing*	Reflections*
$RhHg_2$	36.01	2.4936	2.4980	101
Rh	47.11	1.9290	1.9020	200
$RhHg_2$	54.42	1.6858	1.6850	211
Rh	69.21	1.3574	1.3450	220
$RhHg_2$	69.34	1.3552	1.3600	112
$RhHg_2$	75.64	1.2572	1.2520	202
$RhHg_2$	83.84	1.1539	1.1640	321
Rh	83.90	1.1532	1.1468	311

* From [22]

From all of the experimental interplanar spacings and the lattice parameters (a and c) obtained for an original prototype of $RhHg_2$, the experimental lattice parameters were generated and are shown in Table 3. The differences between the measured

lattice parameterers (a and c) and those reported in the literature [22] are quite significant (parameter a: 0.5%; parameter c: 0.2%). Deviation from stoichioimetry is ruled out as a reason, because the published works indicate that $RhHg_2$ is stable over only a very narrow composition range [23, 24]. The presence of a compressive strain in the amalgam is another possible factor to explain this difference.

Table 3 Comparison of the lattice parameters calculated from experimental data (Table 2) with the prototype of $RhHg_2$

$RhHg_2$/Rh	Lattice parameters	
	$(a \pm \sigma)$ Å	$(c \pm \sigma)$ Å
Prototype*	4.551	2.998
Experimental	4.529±0.002	3.003±0.005
Difference/%	0.5	0.2

* From [22]

Figure 4a depicts mapping surfaces of Rh foils after Hg electrodeposition and heating to a temperature corresponding to the end of the second step. This image reveals the Hg atoms present in higher concentration on the surface of the grain, and in lower concentration at the grain boundaries. These facts are in agreement with the EDX microanalysis results obtained at the same temperature.

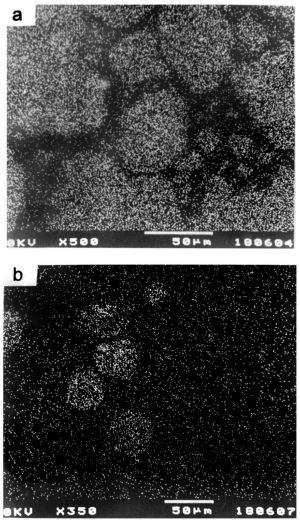

Fig. 4 Mapping of Hg on Rh surfaces foil: a – 175°C, amplification b: 500×; b – 230°C; amplification b: 350×. Electron beam acceleration: 30 kV

For atomic absorption analysis, the foil heated up to 175°C was treated as described in the Experimental section. It is interesting to note that in this solution Rh was detected (Table 1) displaying a surface instability caused by its interaction with Hg. This seems to indicate that the atomic size factor between Hg and Rh may intro-

duce a surface destruction, which can facilitate the attack on the Rh foil surface by the acid solution. As concerns pure Pt, Pt–Rh (10 mass%) and Pt–Ir (20 mass%) alloy, these results and their interpretation are in agreement with [16, 18].

Figures 2c and 2d show SEM images of the surface of Rh foils after Hg electrodeposition and heating to an intermediate temperature (230°C) during the last step in the TG curve and its end (800°C). The Rh surface (Fig. 2c) exhibit grain boundaries, which are not so clearly seen for the Rh surface (Fig. 2b). The image of Fig. 2d reveals a considerable surface roughening. Rh exhibits a morphology that is very different from that shown by Pt, Pt–Rh (10 mass%) and Pt–Ir (20 mass%) [16, 18].

Figure 4b shows the mapping surface of the Rh foil surface after Hg electrodeposition and heating up to 230°C corresponding to an intermediate temperature during the last step in the TG curve. This Fig. reflects a surface cleaner than that in Fig. 4a, as a consequence of Hg elimination by heating, but Hg atoms are still present on the same grains. The EDX microanalysis results confirm the presence of Hg on the Rh foil surface at this intermediate temperature, preferentially on the grains, as seen in Figs 3c,d and 4b. These results are in agreement with those obtained by using atomic absorption analysis (Table 1). Hg was also detected on the surface of Pt–Rh (10 mass%), and Pt–Ir (20 mass%) and pure Pt foils by EDX even when the samples were heated at 600°C. After heating of the samples up to 800°C, only the Pt alloys display Hg on the surface [16, 18]. This behaviour has been attributed to an amalgam formation involving Hg diffusion into the lattice. However, after the Rh foil had been heated up to 250°C, Hg was no longer present according to the EDX microanalysis results (Fig. 3e).

Conclusions

This studies presented here identify Hg film formation on pure Rh foil. This film can be formed by Hg electrodeposition on the metal foil, followed by heating at different temperatures. Hg loss occurs in at least three steps: between room temperature and 160°C, only the bulk Hg is removed; from this temperature up to about 175°C the mass loss can be attributed to the removal of a film of metallic Hg; and finally, between 175 and 230°C, the mass loss step can be ascribed to the desorption of Hg present with a film of $RhHg_2$. EDX microanalyses have proved the presence of Hg on the grain surface after heating up to different temperatures, in agreement with the findings from the TG and DTG curves. The SEM images demonstrate that the grain boundaries are not attacked under specified conditions, possibly because the surface tension of Hg leads to its removal from the grain boundaries. The SEM image for Rh foil at 800°C reveals a considerable surface roughening, which was also observed for the Pt–Rh (10 mass%) alloy [18], but was absent for pure Pt and the Pt–Ir (20 mass%) alloy [16] on heating at the same temperature.

References

1 R. W. Joyner and E. S. Shapiro, Catalysis Letter, 9 (1991) 239.
2 M. B. Kizling, P. Stenius, S. Andersson and A. Frestad, Appl. Catal. B-Environ, 1 (1992) 149.
3 E. Xue, K. Seshan, J. G. Vanommen and J. R. H. Ross, Appl. Catal. B-Environ, 2 (1993) 183.

4 G. E. Poirier, B. K. Hance and J. M. White, J. Phys. Chem., 97 (1993) 5965.
5 J. L. G. Fierro, J. M. Palacios and F. Tomas, J. Mater. Sci., 27 (1992) 685.
6 M. Awada, J. Strojek and G. M. Swain, J. Electrochem. Soc., 142 (1995) L42.
7 M. Fleishmann, S. Pons, D. Robson and P. P. Schmidt (Eds.), Ultramicroelectrodes, Datatech Science Morganton, N. C., 1987.
8 R. M. Whightmann and D. O. Wipf, in A. J. Bard (Eds.), Electroanalytical Chemistry, Vol. 15, Marcel Dekker, New York 1989.
9 P. J. Cumpson and M. P. Seah, National Physical Laboratory (UK), Internal communication 1994, p. 32.
10 C. Guminski, Bull. Alloy Phase Diagrams, 11 (1990) 22.
11 T. B. Massalski, H. Okamoto, P. R. Subramanian and L. Kacprzak (Eds.), Binary Alloy Phase Diagrams, ASM, International Press, USA 1990, Vol. 3.
12 S. P. Kounaves and J. Buffle, J. Electroanal. Chem., 216 (1987) 53.
13 M. Z. Hassan, D. F. Untereker and S. Bruckenstein, J. Electroanal. Chem., 42 (1973) 161.
14 S. Affrossman and W. G. Erskine, Trans. Faraday Soc., 62 (1966) 2922.
15 S. Affrossman, W. G. Erskine and J. Paton, Trans. Faraday Soc., 64 (1968) 2856.
16 F. L. Fertonani, A. V. Benedetti and M. Ionashiro, Thermochim. Acta, 265 (1995) 151.
17 G. D. Robins and C. G. Enke, J. Electroanal. Chem., 23 (1969) 343.
18 F. L. Fertonani, M. Ionashiro, P. Melnikov, F. Sanz and A. V. Benedetti, Thermochim. Acta – to be submitted.
19 C. Feldman, Anal. Chem., 46 (1974) 99.
20 E. Jackwert, P. G. Willmer, R. Höhn and H. Berndt, At. Abs. Newsl., 18 (1979) 66.
21 C. Wechter and J. Osteryoung, Anal. Chim. Acta, 234 (1990) 275.
22 Powder Diffraction File PDF2, Data Base Sets 1–44, published by the Joint Committee on Powder Diffraction Standard – International Centre for Diffraction Data, Pennsylvania, 1988 (CD-ROM).
23 M. Hansen, Constitution of Binary Alloys, McGraw-Hill, New York 1958.
24 G. Jangg and T. Dortbudak, Z. Metallkd., 64 (1973) 715.
25 F. L. Fertonani, A. V. Benedetti, J. Servat, J. Portillo and F. Sanz, Thin Solid Films, 341 (1999) 1.